

# A liquid-supported condensation of major minerals in the solar nebula: Evidence from glasses in the Kaba (CV3) chondrite

M.E. Varela<sup>a,\*</sup>, G. Kurat<sup>b</sup>, E. Zinner<sup>c</sup>

<sup>a</sup> CONICET, Universidad Nacional del Sur, Departamento de Geología, San Juan 670, B. Blanca, Argentina

<sup>b</sup> Institut für Geologische Wissenschaften, Universität Wien, Althanstrasse 14, A-1090 Vienna, Austria

<sup>c</sup> Laboratory for Space Sciences and Physics Department, Washington University, St. Louis, MO 63130, USA

Received 16 December 2004; revised 12 April 2005

Available online 1 July 2005

## Abstract

Glasses, in the Kaba CV3 chondrite, occur as mesostasis in chondrules and aggregates and as inclusions in olivines, both confined or open and connected to the mesostasis. The inclusions in olivine and the glassy mesostasis of aggregates seem to have formed contemporaneously. The confined glass inclusions and open inclusions in olivine were formed during olivine growth and the mesostasis glass during olivine aggregation. All glasses have high trace element contents ( $10\text{--}20 \times \text{CI}$ ) with unfractionated CI-normalized abundances of refractory trace elements. In contrast, V, Mn, Li, and Cr are depleted in all glasses with respect to the refractory trace elements, as is Rb in the glass inclusions in olivine but not in the mesostasis glass. This abundance pattern indicates vapor fractionation and a common condensation origin for both glasses. Glasses of confined glass inclusions in olivine have a Si–Al–Ca-rich composition with a chondritic Ca/Al ratio. Glasses of open glass inclusions and mesostasis are poor in Ca and enriched in alkalis. However, Ca contents of olivines indicate crystallization from a Ca-rich melt of a composition similar to that of the glass inclusions. In addition, trace element abundances indicate that these glasses (liquids) probably had an original composition similar to that of the inclusion glass. They apparently lost Ca in exchange for alkalis in a metasomatic exchange reaction, presumably with the vapor. There is now growing evidence that liquids can indeed condense from a solar nebula gas, provided the gas/dust ratio is sufficiently low. In these regions with enhanced oxygen fugacity as compared to that of a nebula of solar composition, liquids (the glass precursor) probably played an important role in growing crystals from the vapor by liquid-phase epitaxy. The glasses appear to be the remnants of this thin liquid layer interface that supported the growth of olivine from the vapor following the Vapor–Liquid–Solid process. This liquid will have a refractory composition and will have trace element contents which are in equilibrium with the vapor, and, therefore, will not change much during the time of olivine growth. The composition of the liquid seems to be unconstrained by the phases it is in contact with. Samples of this liquid will be retained as glass inclusions in olivine. The glassy mesostasis could also be a sample of this liquid that got trapped in inter-crystal spaces. The mesostasis glass subsequently behaved as an open system and its Ca was exchanged—presumably with the vapor—for the alkali elements Na, K, and Rb. In contrast, glass inclusions in olivine were protected by the host, could not react, and thus preserved the original composition of this liquid.

© 2005 Elsevier Inc. All rights reserved.

**Keywords:** Cosmochemistry; Solar nebula; Meteorites

## 1. Introduction

Since Fuchs et al. (1973) reported the first Ca–Al-rich glass inclusions in olivines of the Murchison carbonaceous

chondrite, several models have been proposed to explain their origin. One of these models considers olivines to be a crystallization product of chondrule melts (Richardson and McSween, 1978; McSween, 1977) and thus sees glasses in minerals of aggregates and chondrules as parental melts trapped during olivine crystallization and the mesostasis glass as a residual melt after olivine crystallization (McSween, 1977; Roedder, 1981). A second model consid-

\* Corresponding author.

E-mail addresses: [evarela@criba.edu.ar](mailto:evarela@criba.edu.ar) (M.E. Varela), [gero.kurat@univie.ac.at](mailto:gero.kurat@univie.ac.at) (G. Kurat), [ekz@wustl.edu](mailto:ekz@wustl.edu) (E. Zinner).

ers olivines to be high temperature nebular condensates (e.g., Larimer and Anders, 1967; Grossman, 1972) and glass inclusions are seen as a product of the condensation process (Fuchs et al., 1973). This latter view gained strength when the first trace element analyses of glass inclusions in olivine of a carbonaceous chondrite favored an origin by condensation (Kurat et al., 1997). Recently, a study of the chemistry of glass inclusions in olivines in the CR chondrites indicated that glass inclusions could be seen as remnants of liquids that were trapped when the olivine formed by condensation from the vapor (Varela et al., 2002). Thus, glass inclusions in olivines of carbonaceous chondrites could represent primitive (condensate) liquids (Yoneda and Grossman, 1995). Therefore, and considering that for both models glass inclusions represent remnants of a liquid, the question that arises is: what is the difference between them? The difference resides in the role of this primitive liquid. The comprehension on how that liquid can be generated and its role is crucial to understand the subsequent processes. Because of this, we will extensively discuss this point later and only a summary is given here.

While in the conventional model *crystals are grown from a droplet* of liquid (commonly called “melt”) of chondritic composition, in our model the Si–Al–Ca liquid *serves as a support to grow* crystals (e.g., olivine, pyroxene, plagioclase) directly from the vapor. In our view, glass inclusions represent remnants of the thin liquid layer that helped olivine to grow from the vapor (Kurat et al., 1997; Varela et al., 2002). Thus, the chemical composition of this liquid preserved in glass-bearing inclusions in minerals reflects processes in the early solar nebula: condensation and in some cases also post-formational glass–vapor exchange reactions. An example of such nebular alteration are some glass inclusions in olivines of CR chondrites. Their chemical composition appears to be pristine except for the presence of alkalis (mainly Na) and the moderately volatile elements Cr, V, and Mn, which possibly were acquired by solid–vapor exchange (Varela et al., 2002). Another example of nebular alteration are glasses in the angrite D’Orbigny whose chemical compositions reflect their behavior as both, closed and open systems (Varela et al., 2003b). Thus, glasses can record changing conditions prevailing during and after their formation (e.g., Kurat, 1967).

The physico-chemical conditions under which silicate liquids can condense in a dust-enriched system were predicted for Ca-rich glasses (Ebel and Grossman, 2000) but there is no prediction for Na-rich glasses such as those commonly present in Type I chondrules.

Here we report on a study of glass inclusions in olivine of the Kaba CV3 chondrite and glass inclusions in olivine and glassy mesostasis co-existing in a Kaba aggregate. The results suggest that both glasses could have a similar—nebular—origin and thus, represent a sample of the initial refractory liquid that helped to grow crystals from the vapor.

## 2. Analytical techniques and samples

Glass inclusions in olivines were studied with the optical microscope in order to establish their occurrence and textural relationships with host olivines grains constituting aggregates or chondrules.

Major element chemical compositions of glasses and hosts were obtained with a JEOL 6400 analytical scanning electron microscope (NHM, Vienna) and SX100 and SX50 CAMECA electron microprobes (Institute of Geological Sciences, University of Vienna, and Atomic Energy Commission of Argentina, Buenos Aires, respectively). Microprobe analyses were performed at 15 kV acceleration potential and 10 nA sample current. Analyses of minerals and glasses were performed using a focused beam ( $\sim 1 \mu\text{m}$ ) and a defocused beam ( $5 \mu\text{m}$ ), respectively. The samples were first analyzed for Na with a counting time of 5 s followed by all other elements with a counting time of 10 s. These analytical conditions prevent premature Na loss from glasses. The precision was established by analyzing basaltic and trachytic glasses (ALV 981 R24 and CFA 47; Métrich and Clochiatti, 1989) and corrections were made using the on-line ZAF program.

Trace element analyses of glasses of glass inclusions, glass mesostasis and host olivines were made with the Cameca IMS 3F ion microprobe at Washington University, St. Louis, following a modified procedure of Zinner and Crozaz (1986).

The samples studied are in the Polished Thin Sections (PTS) “Kaba L3819,” “Kaba from A576,” and “Kaba M4816” (all from the NHM, Vienna).

## 3. Results

### *Petrography and major element content of glasses and host olivines*

Before beginning this section we need to present the definitions used to distinguish chondrules from aggregates, and that applied to one type of glass object.

**Chondrules:** Round, droplet-shaped objects that have apparently been at least partly liquid in the course of their history (“droplet chondrule” in American terminology, e.g., Gooding and Keil, 1981).

**Aggregate:** An irregularly shaped angular to rounded aggregation of minerals with or without supporting mesostasis.

**Neck inclusions:** These are open glass inclusions in olivine that are still connected by a neck or umbilical cord to the mesostasis. They are inclusions *in statu nascendi* and generally located near the surface of the olivine. In these glasses the typical shrinkage bubble, the result of a volume decrease at the liquid-glass transition, is missing, as these glasses are not in a closed system. Their chemical composition is usually very similar to that of the mesostasis but we shall distinguish them from the mesostasis be-

cause these glasses are not filling the interstitial space in between different phases but instead are included in a single one.

All studied glass inclusions in olivine are primary inclusions (for definition see Varela et al., 2002), consist of clear glass and a bubble and vary in size from 8 to 30  $\mu\text{m}$ .

Glass inclusions generally occur isolated. Only rarely were clusters of glass inclusions observed in olivines of aggregates in the PTS Kaba from A576 (inclusions 5, 6, 7, and 18, Fig. 1B, Table 1) and in the PTS Kaba M4816 where glass inclusions 9 and 10 co-exist in an aggregate that consists of three olivine grains with scarce mesostasis (Fig. 1A, Table 1). The particular opportunity to study a clear glassy mesostasis was presented by the PTS Kaba L3819. In this sample, a primary glass inclusion in olivine (inclusion 12, Table 1; encircled in Fig. 2B) and the clear glassy mesostasis (Tables 1 and 2, Fig. 2C) co-exist in an aggregate with porphyritic texture (Figs. 2A, 2B, 2E).

Another type of glass considered in this study are neck inclusions (e.g., f and e, Figs. 2C, 2D). Neck inclusions c and d (Table 1) co-exist in the same host olivine with glass inclusions 5, 6, 7, and 18. Neck inclusions f and e (Table 1, Fig. 2C) co-exist in a porphyritic aggregate with the glassy mesostasis and the glass inclusions 12 and 21 (Figs. 2A, 2B, 2E).

All glass inclusions labeled in Table 1 “glass inclusions with fractures” are in contact with one fracture, with exception of glass inclusion 18, which is in contact with three (Fig. 1B).

Host olivines of all glasses form parts of chondrules or aggregates with porphyritic olivine (PO), porphyritic olivine-pyroxene (POP) and equigranular olivine (EO) texture. One host olivine belongs to an aggregate dominated by a barred olivine and several subhedral olivine crystals (BO + PO, in Table 1). Two host olivines (host of glass inclusions 13 and 14, Table 1) belong to an aggregate formed by a barred olivine chondrule in the center and several anhedral olivines attached to it (Figs. 3A, 3B, 3C).

All inclusion glasses are Si–Al–Ca-rich with approximately chondritic Ca/Al and subchondritic Ti/Al ratios and low Na<sub>2</sub>O contents (<1.5 wt%) (Table 1, Figs. 4, 5).

Glasses of inclusions in contact with fractures cover the same compositional range as those without fracture links with the exception of Na<sub>2</sub>O, which is abundant (up to 6.7 wt%, Fig. 6) and CaO, which is less abundant than in inclusions that are not in contact with fractures (down to 8.2 wt% in glass inclusion 18, Table 1 and Fig. 6). The glass compositions of the neck inclusions and the glassy mesostasis cover a similar range in Al<sub>2</sub>O<sub>3</sub> and Cr<sub>2</sub>O<sub>3</sub> contents as those of the inclusion glasses. These glasses are at the lower compositional range in TiO<sub>2</sub> contents (0.31 to 0.72 wt%), have low contents of CaO (3.9 to 10.3 wt%) (Fig. 6), have high contents of FeO (0.94 to 2.96 wt%, with the exception of the glass of the neck inclusion that has 0.16 wt%), and are very rich in Na<sub>2</sub>O (6.1 to 8.9 wt%) and K<sub>2</sub>O (0.12 to 0.57 wt%) (Table 1 and Figs. 6, 7). Nuclear microprobe

analysis of glass inclusions 5, 6, and 7 showed that glasses have variable contents of nitrogen and (carbon): 200 ppm (610 ppm), 30 ppm (2090 ppm), 190 ppm (250 ppm), respectively (Varela et al., 2000, 2003a).

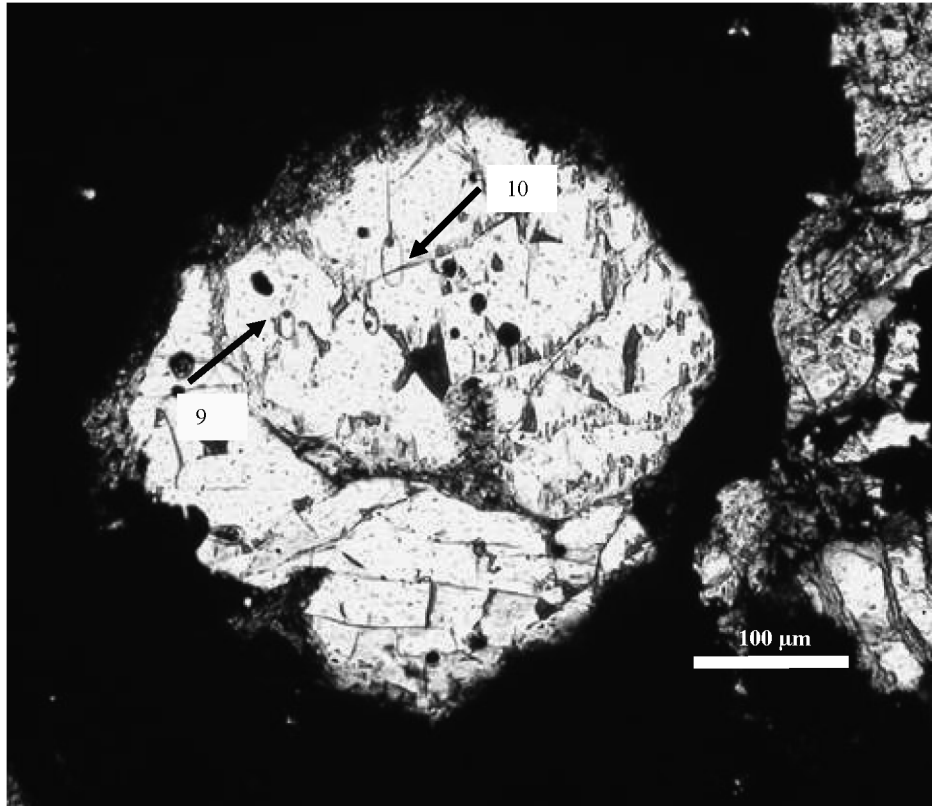
Host olivines of glass inclusions, of neck inclusions and olivines that are in contact with the glassy mesostasis (labeled as a, b, c, and d in Table 1 and Fig. 2C), have FeO contents varying from 0.32 to 1.5 wt% (with exception of the host olivine of the glass inclusion 15 that has a FeO content of 4.5 wt%) and CaO contents of 0.06 to 0.54 wt% (Table 1). Pyroxene in the PTS Kaba L3819 (Figs. 2A, 2B) is a typical low-Ca pyroxene of carbonaceous chondrites (SiO<sub>2</sub>: 58.7 wt%, Al<sub>2</sub>O<sub>3</sub>: 1.1 wt%, Cr<sub>2</sub>O<sub>3</sub>: 0.5 wt%, FeO: 0.5 wt%, MgO: 38.1 wt% and CaO: 0.4 wt%).

Trace element abundances of inclusion glasses are high and typical at 10–20  $\times$  CI abundances (Figs. 9, 10). Using Si as internal standard, SIMS data of inclusion glasses show a deficit in Ca content as compared to the EMP data, which is probably due to some dilution from the underlying olivine. This contamination has only slightly increased the V, Mn, and Cr content but has considerably affected the Ca content of these glasses. Consequently, the inclusion data were re-normalized to the Ca content as determined by EMP. Analyses of neck inclusion and mesostasis glasses do not show such dilution effect. The Ca contents of these glasses measured by SIMS and EMP are similar, therefore the original Si-normalization was kept.

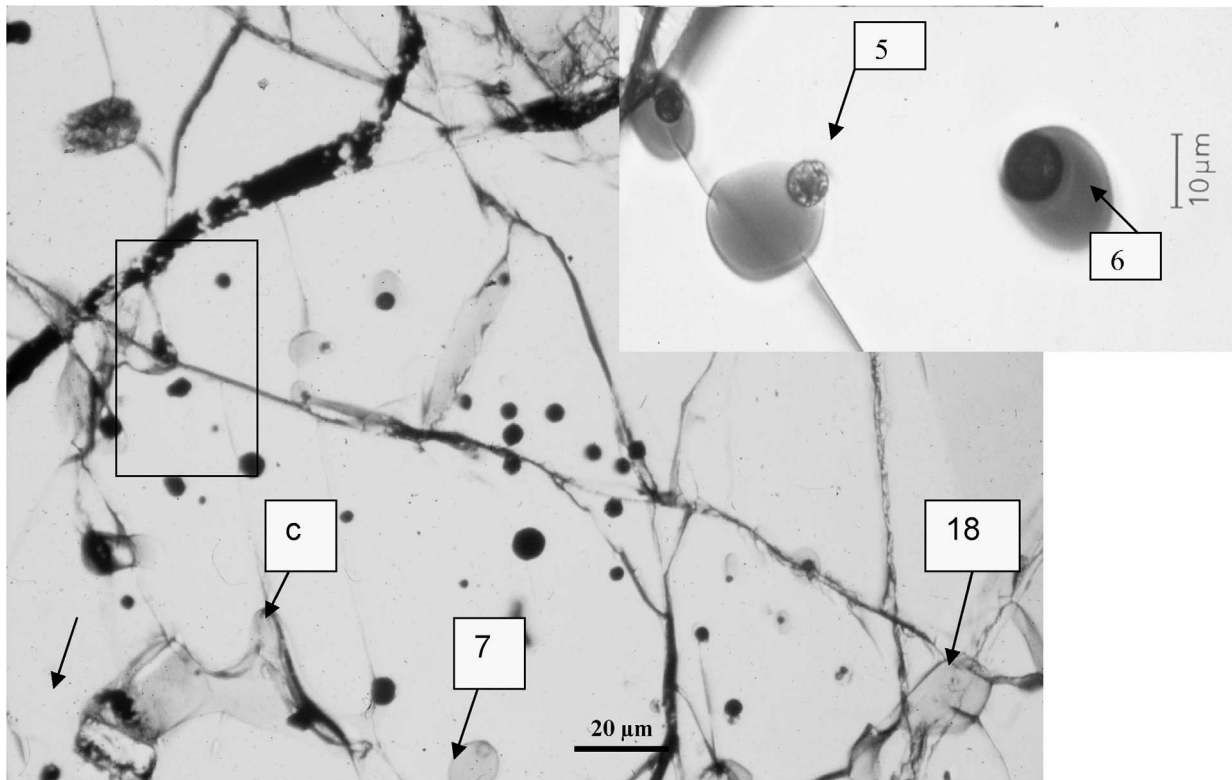
#### 4. Discussion

In a previous contribution, based on the chemistry of glass inclusions in olivines of CR chondrites (Varela et al., 2002), we proposed a model of formation of glass inclusions based on the concept that glasses are the possible remnants of the liquid interface between growing crystal and the vapor. However, we were not able to address the subject of the mesostasis glasses in chondrules at that time. All the aggregates and chondrules in the studied CR chondrites had crystallized mesostasis that did not allow us to obtain useful analyses for comparison with those of the glass inclusions. Chondrules and aggregates containing olivines with primary glass inclusions that co-exist with glassy mesostasis are scarce. This is even more rare in the case of CV chondrites where commonly chondrules and aggregates do not contain glassy mesostasis, but consist of holocrystalline assemblages, mainly of plagioclase and Ca-rich pyroxene, that are usually altered (e.g., Ikeda and Kimura, 1995). However, the study of primary glass inclusions in olivines of several chondrules and aggregates as well as the study of an aggregate where all glasses co-exist in a glassy state (glassy primary glass inclusions, neck inclusions and mesostasis) in the Kaba CV3 chondrite gives us the opportunity to advance in the previously unsolved issue.

In the following part of this section we will introduce the reader with the way liquids can be produced in the solar neb-



(A)



(B)

Fig. 1. (A) Transmitted light image of an aggregate in Kaba (PTS Kaba M4816) formed by three olivines and scarce mesostasis. Arrows indicate locations of glass inclusions 9 and 10. (B) Transmitted light image of the olivine in Kaba (PTS Kaba von A576) showing the co-existence of glass inclusions 5, 6, 7, and 18 and the neck inclusion c. Arrow in the left corner signals the location of the neck inclusion d. A detail of the rectangular area shows glass inclusion 5 and 6.

Table 1

Major element composition of glasses of glass inclusions in olivines, of neck inclusions and of glass mesostasis in chondrules of Kaba carbonaceous chondrite (electron microprobe analysis in wt%)

Glass inclusions without fracture												
	1	2	3	4	6	7	8	9*	11	12*	13	14*
SiO <sub>2</sub>	52.9	47.8	42.2	42.6	42.0	42.7	56.9	49.4	53.6	52.3	51.8	46.9
TiO <sub>2</sub>	1.02	1.12	1.13	0.65	1.06	0.99	0.38	0.98	0.65	0.94	0.89	0.90
Al <sub>2</sub> O <sub>3</sub>	20.4	21.0	29.4	25.8	29.2	28.7	20.2	24.8	23.5	23.0	24.0	25.0
Cr <sub>2</sub> O <sub>3</sub>	0.19	0.30	0.27	0.69	0.26	0.16	0.10	0.32	0.29	0.35	0.40	0.20
FeO	0.29	0.22	0.14	1.99	0.28	0.15	0.09	0.28	0.22	0.26	0.68	0.29
MnO	0.01	0.11	0.00	0.00	0.01	0.02	0.10	0.00	0.10	0.06	0.06	0.00
MgO	4.92	9.9	3.25	5.9	3.20	3.62	3.11	3.70	3.54	3.68	3.24	3.43
CaO	20.0	17.6	23.4	19.2	23.9	22.6	18.6	19.9	18.1	18.2	17.8	22.5
Na <sub>2</sub> O	0.00	0.00	0.03	0.01	0.02	0.00	0.04	0.11	0.05	1.07	1.23	0.69
K <sub>2</sub> O	0.03	0.00	0.00	0.01	0.00	0.00	0.05	0.00	0.00	0.01	0.01	0.00
P <sub>2</sub> O <sub>5</sub>	0.20	0.16	0.29	0.17	0.28	0.30	0.22	0.00	0.05	0.13	n.d.	n.d.
Total	99.9	98.3	100.2	96.9	100.3	99.3	99.7	99.5	100.0	100.0	100.0	100.0
Ol. host												
FeO	0.65	0.42	0.12	0.40	0.32	0.32	0.60	0.50	0.30	0.78	0.93	0.30
CaO	0.35	0.32	0.58	0.41	0.54	0.54	0.36	0.30	0.36	0.25	0.30	0.36
Texture	MO	BO + PO	PO	PO	PO	PO	POP	PO	PO	POP	BO + PO	BO + PO
	Ch.	Agg.	Agg.	Agg.	Agg.	Agg.	Agg.	Agg.	Agg.	Agg.	Agg.	Agg.
Glass inclusions with fractures												
	5	10*	15	16	17	18	19	20	21			
SiO <sub>2</sub>	40.9	51.4	55.8	53.7	55.6	53.6	50.3	54.8	56.9			
TiO <sub>2</sub>	0.88	0.89	0.67	1.28	0.39	0.74	0.51	1.13	0.51			
Al <sub>2</sub> O <sub>3</sub>	30.5	23.6	20.2	18.6	18.5	21.9	22.3	23.5	21.1			
Cr <sub>2</sub> O <sub>3</sub>	0.09	0.30	0.29	0.16	0.23	0.29	0.03	0.17	0.44			
FeO	0.24	0.22	1.60	0.13	0.90	3.95	0.50	0.13	0.29			
MnO	0.00	0.02	0.00	0.00	0.06	0.11	0.00	0.03	0.1			
MgO	3.42	3.61	2.99	3.68	3.42	3.47	3.48	2.70	1.7			
CaO	23.6	19.7	15.4	20.8	16.7	8.2	21.0	17.3	14.8			
Na <sub>2</sub> O	0.00	0.00	2.99	0.04	2.91	6.69	0.00	0.58	4.26			
K <sub>2</sub> O	0.00	0.02	0.08	0.00	0.04	0.34	0.00	0.09	0.04			
P <sub>2</sub> O <sub>5</sub>	0.26	0.02	0.18	0.23	0.23	0.07	0.24	0.25	0.3			
Total	99.9	99.8	100.2	98.6	99.0	99.4	98.4	100.6	100.4			
Ol. host												
FeO	0.32	0.50	4.50	0.60	0.70	0.32	0.34	0.50	0.69			
CaO	0.54	0.30	0.30	0.30	0.30	0.54	0.06	0.22	0.26			
Texture	PO	PO	PO	PO	PO	PO	POP	POP	POP			
	Agg.	Agg.	Agg.	Agg.	Agg.	Agg.	Agg.	Agg.	Agg.			
Neck inclusions					Glassy mesostasis in aggregate L3819							
	c	d	e	f*	1	2	3	4	5			
SiO <sub>2</sub>	57.0	55.7	56.2	55.6	56.1	56.5	56.6	55.3	55.7			
TiO <sub>2</sub>	0.72	0.36	0.55	0.43	0.48	0.54	0.50	0.37	0.40			
Al <sub>2</sub> O <sub>3</sub>	21.3	21.7	25.0	26.5	24.3	24.8	25.7	24.1	23.1			
Cr <sub>2</sub> O <sub>3</sub>	0.37	0.22	0.28	0.33	0.13	0.19	0.17	0.40	0.51			
FeO	0.94	1.57	0.96	1.53	2.17	1.89	2.40	1.17	1.28			
MnO	0.03	0.11	0.03	0.05	0.04	0.03	0.04	0.03	0.01			
MgO	3.07	2.85	2.24	1.70	2.98	2.64	1.71	3.47	3.97			
CaO	9.7	10.0	5.50	4.71	4.59	4.56	3.91	5.8	6.3			
Na <sub>2</sub> O	7.4	6.9	8.6	8.7	8.8	8.3	8.4	8.9	8.3			
K <sub>2</sub> O	0.12	0.15	0.47	0.47	0.45	0.50	0.57	0.40	0.36			
P <sub>2</sub> O <sub>5</sub>	0.04	0.11	0.00	0.00	0.00	0.00	0.00	0.00	0.00			
Total	100.6	99.7	99.9	100.0	100.0	99.9	100.0	100.0	100.0			
Ol. host					Ol.	a	b	c	d			
FeO	0.32	0.32	0.73	0.73	FeO	0.73	0.95	0.78	0.78			
CaO	0.54	0.54	0.25	0.25	CaO	0.25	0.48	0.23	0.26			

\* Glass inclusions with secondary mass spectrometry analyses. Figs. 1 (A–B), 2 (A, B, C, D, E), and 3 (A, B) show locations of glass inclusions, neck inclusions, and mesostasis in Kaba samples (PTS M4816, von Kaba A576, L3819).

Table 2

Trace element contents in glasses of glass inclusions and olivine of the Kaba CVS chondrite. Secondary-ion mass spectrometry (SIMS) data in ppm

Element	G.I.12	Error*	Ol.-12	Error	G.I.9	Error	G.I.10	Error	Ol.-9-10	Error	G.I.14	Error
Li	0.33	0.09	0.4	0.04	3.7	0.2	6.7	0.6	1.08		2.16	
Be	0.56	0.09			0.48		0.43	0.04			0.57	
B	2.23	0.40	0.13	0.02	0.82	0.09	1.3	0.2	0.134	0.018	4.47	
Sc	42.3		3.7		42.7		40		3.32		36.9	
Ca	129900		1400	66	141750		140600		1560	33	160200	
Ti	5780		124		5982		5232		165		5452	
V	123.5		93.9		67.7		108.2		82.6		79.5	
Cr	3363		1970		3428		4150		1815		2530	
Mn	542		500		324		405		165		300	
Co	10.6	1.80	1.98	0.29	15		11.8		1.9		3800	
Rb	0.33	0.30									5.22	0.6
Sr	140		0.1	0.01	120		124		0.05	0.007	172	
Y	22		0.07	0.02	24.4		24.7		0.12	0.008	30	
Zr	71.2		0.03	0.008	85		84.8		0.2	0.02	113	
Nb	5	0.86	0.01	0.004	3.32		3.15		0.006	0.002	4.7	
Ba	44		0.13	0.02	31.5		34.4		0.04	0.008	48.6	
La	3.86	0.60			3.38	0.2	5.4		0.006	0.002	6.13	
Ce	9.3	1.30	0.0046	0.002	11.5		11.8		0.01	0.003	15.7	
Pr	1.4	0.24			1.73	0.1	1.87	0.09			2.4	
Nd	5.35	0.40			8.48		7.93				11.9	
Sm	2.37	0.15	0.01	0.005	1.54		1.25	0.13			2.35	
Eu	0.69	0.48			0.77		0.87	0.04			1.15	
Gd	2.6	0.53	0.025	0.008	3.78	0.42	3.53	0.4			4	0.4
Tb	0.77	0.22	0.0048	0.002	0.64	0.07	0.68	0.1			0.75	0.07
Dy	3.3	0.48	0.09	0.01	4.36		5		0.006	0.002	5.75	
Ho	0.56	0.14	0.019	0.005	0.93	0.09	1.18	0.1	0.004	0.001	1.1	0.09
Er	2.34	0.30	0.067	0.01	3		2.9		0.015	0.003	3.57	
Tm	0.3	0.08	0.015	0.004	0.3	0.04	0.39	0.04			0.5	0.05
Yb	2.17	0.67	0.11	0.03	2.55		2.21		0.03	0.005	2.37	0.22
Lu	0.33	0.11			0.33	0.06	0.45	0.06	0.006	0.002	0.43	0.05
Element	Neck inclusion	Error*	Mesostasis 1	Error	Mesostasis 2	Error	Mesostasis 3	Error				
Li	0.29		0.34		0.24		0.32					
Be	0.54		0.75		0.64		0.66					
B	0.68		0.42		1.09		34					
Sc	22.5		22.9		21.8		20.2					
Ca	39600		38000		46500		31900					
Ti	2470		2480		2260		2020					
V	32		16		16		43					
Cr	1840		1140		2175		716					
Mn	487		290		198		616					
Co	4.9		36.9		8.46		30					
Rb	12		19.8		8.35		35.4					
Sr	70		60.6		85.8		86.4					
Y	18.8		20.3		18.4		20.9					
Zr	61.8		74.3		66.4		102.3					
Nb	5.5		5.1		5.9		9.96					
Ba	27.2		21.4		27.3		26.9					
La	3.1		3.6		3.7		5.77					
Ce	9		10.9		9.42		13.9					
Pr	1.33		1.52		1.2		2.1					
Nd	5.9		7		5.7		7.8					
Sm	1.5	0.15	1.75		1.58		2.1					
Eu	0.5	0.05	0.48		0.79		0.27					
Gd	2.1		2.5		1.94		1.96					
Tb	0.41	0.04	0.39	0.04	0.38	0.04	0.51	0.07				
Dy	2.5		3.02		2.32		2.54					
Ho	0.58		0.57		0.47		0.54					
Er	1.56		1.79		1.41		1.79					
Tm	0.24		0.25	0.03	0.2	0.02	0.2	0.03				
Yb	1.54		1.68	0.20	1.35	0.11	1.7	0.22				
Lu	0.2	0.03	0.3	0.03	0.25	0.03	0.21	0.03				

\* Errors are 1 $\sigma$  measurement errors based on counting statistics. They are given only if they exceed 10%, the typical value for systematic errors.

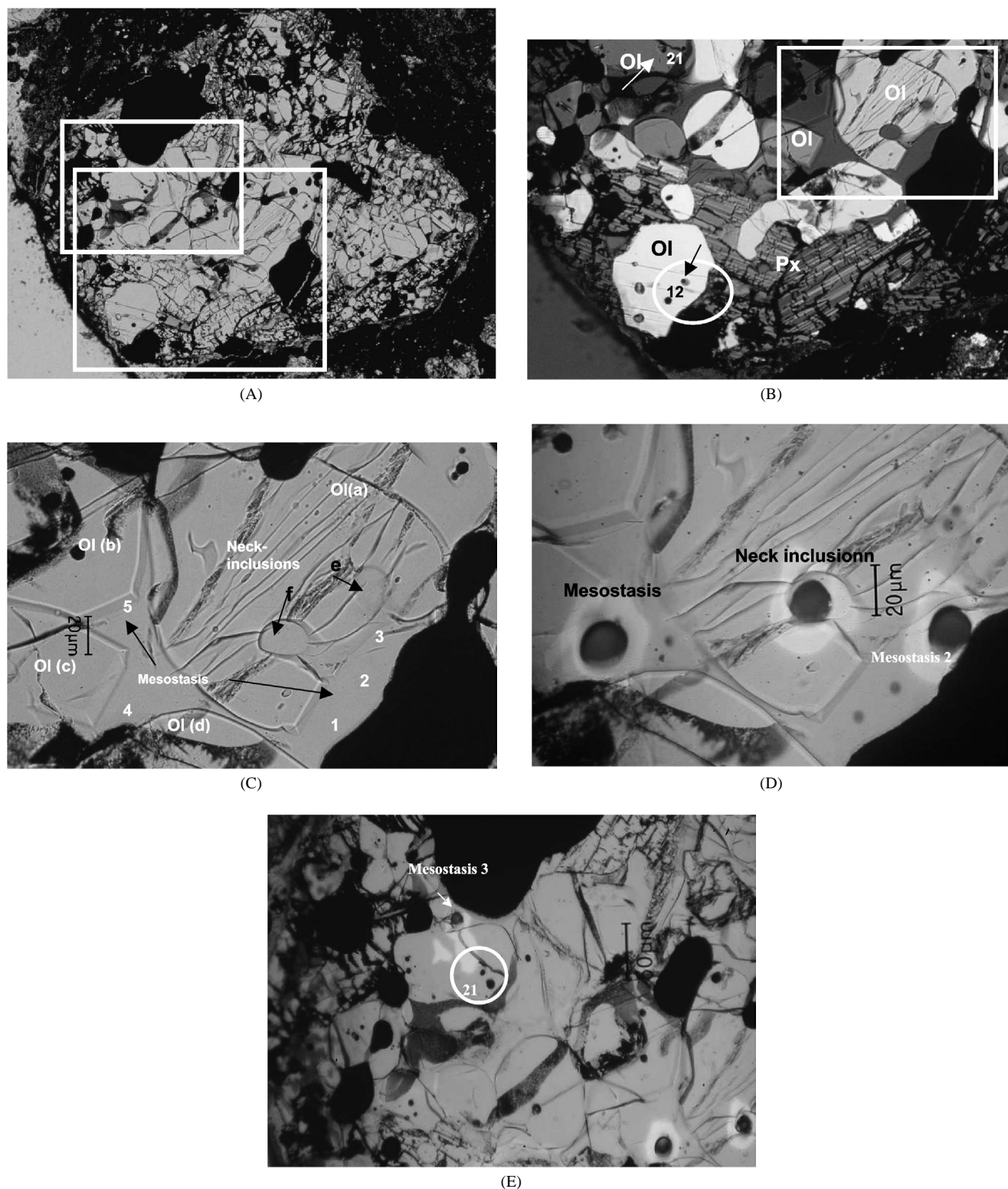
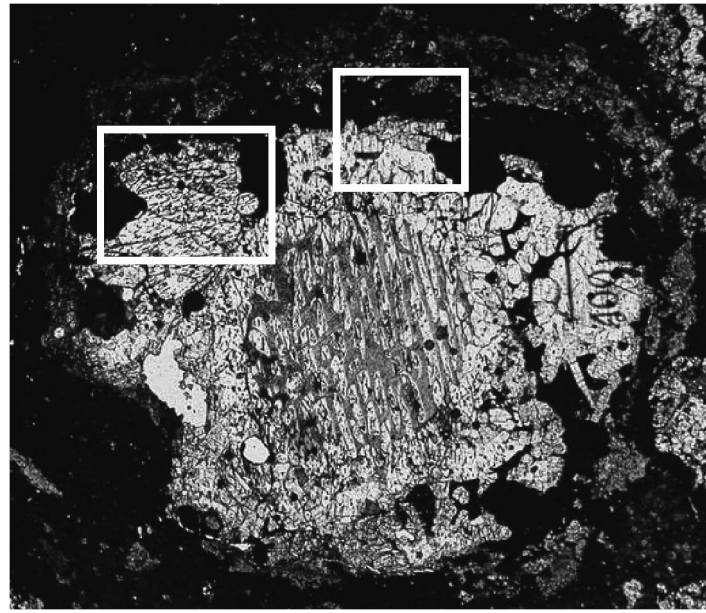
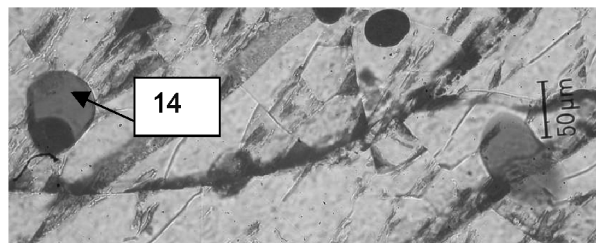


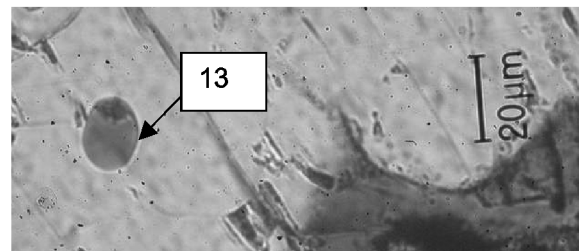
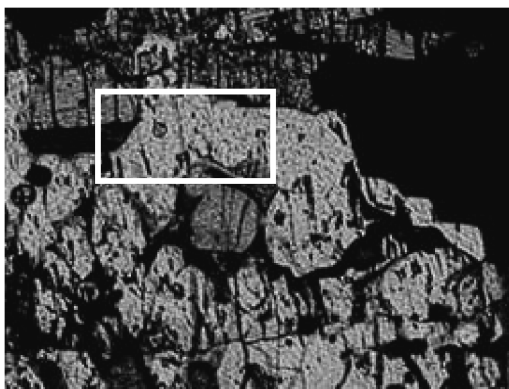
Fig. 2. (A) Transmitted light image of an aggregate in Kaba (PTS Kaba von A576) with a porphyritic olivine–pyroxene texture. Total length of the picture is 1150  $\mu\text{m}$ . (B) Detailed transmitted light image of the big rectangular area indicated in figure (A) showing pyroxenes (twinned, Px) and olivines (Ol), glass inclusion 12 with shrinkage bubble (encircled, black arrow), the glass inclusion 21 with fracture (white arrow upper left corner) and mesostasis glass (abundant within the marked rectangle). Total length of the picture 600  $\mu\text{m}$ . (C) Detailed transmitted light image of the rectangular area of figure (B) showing neck inclusions f and e in olivine and mesostasis glass. Note the clear glassy aspect of the mesostasis glass. Label as Ol (a, b, c, and d) are the olivines in contact with the mesostasis and the numbers 1, 2, 3, 4, and 5 correspond to the location of EMP analysis in the mesostasis (Table 1). Total length of the picture: 240  $\mu\text{m}$ . (D) Same image as figure (C) showing the ion microprobe ablation pits of the neck inclusion and Mesostasis 1 and 2 (Table 2). (E) Detail transmitted light image of the small rectangular area indicate in figure (A) showing the location of glass inclusion 21 and the ion microprobe ablation pit of Mesostasis 3.



(A)



(B)



(C)

Fig. 3. (A) Transmitted light image of an aggregate in Kaba (PTS Kaba von A576) formed by a barred olivine chondrule in the center and several anhedral olivines in the external rim. (B) Detail of the left rectangular area as indicate in figure (A) showing the location of glass inclusion 14 and an enlargement of the inset. (C) Detail of the rectangular area in the center of figure (A) showing the location of glass inclusion 13 and an enlargement of the inset.

ula and update our view of these liquids and their specific role. Next, and after a brief discussion to clarify the concepts of glass inclusions and mesostasis, we discuss all the

results obtained in the glasses of the Kaba CV3 chondrite that give additional support to the role liquids can have in specific regions of the solar nebula.

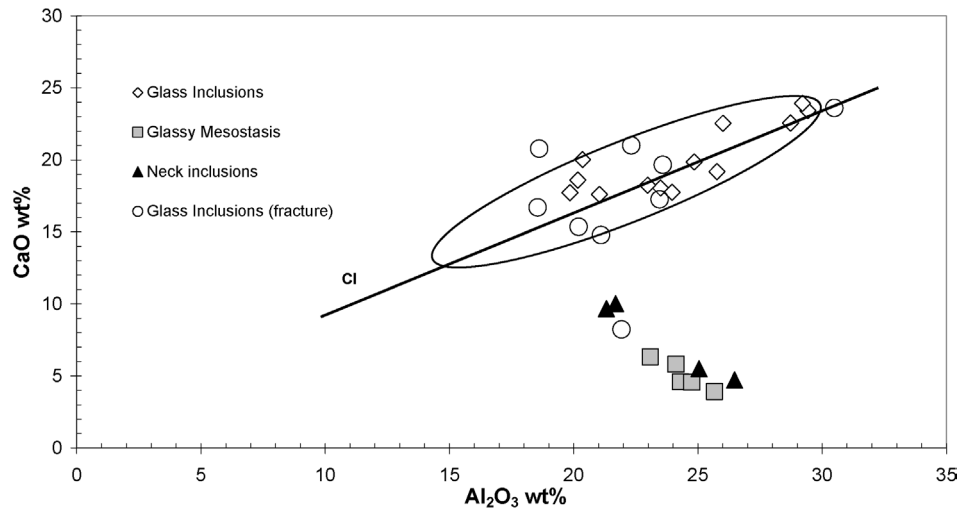


Fig. 4. CaO vs  $\text{Al}_2\text{O}_3$  diagram of all types of glasses encountered in the Kaba CV3 chondrite. Glasses of glass inclusions have a chondritic Ca/Al ratio. Note the Ca-depletion in glasses of the neck inclusions and in the glassy mesostasis relative to the inclusion glasses. The ellipse covers the compositional range of glasses in CR chondrites.

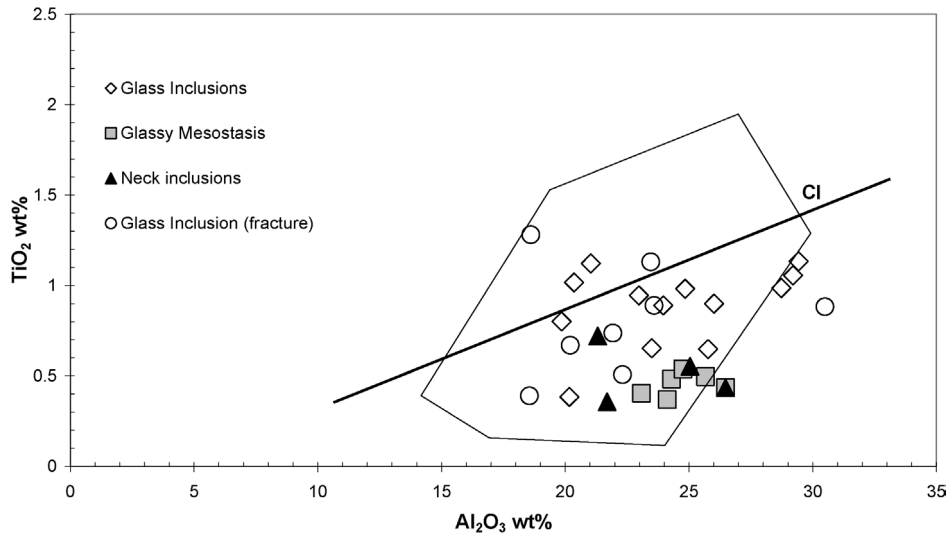


Fig. 5.  $\text{TiO}_2$  vs  $\text{Al}_2\text{O}_3$  diagram of all types of glasses encountered in the Kaba CV3 chondrite. Note that most glasses have sub-chondritic Ti/Al ratios and cover a similar compositional range as glasses (area) in CR chondrites.

#### 4.1. Liquids in the nebula: their possible function in regions with enhanced dust/gas ratios

As it was summarized before, liquids in the solar nebula can be produced either by melting of pre-existing solid matter or by condensation. In order to form chondrules, it is necessary to form a liquid either by condensation or by melting of solid precursors (e.g., Grossman and Wasson, 1982, 1983) and crystallize it later during cooling. In the case of melts derived from solid precursors, glass inclusions will represent a sample of the melt from which crystals are growing and the mesostasis, the residual melt. The chemical composition of these melts changes in the course of crystallization and, if trapped at different stages of the evolution of the chondrule, shall reflect its composition at that particular moment. We

shall expect to find a continuous evolution of the inclusion melt composition up to the final residual mesostasis melt.

Liquids generated by condensation from a gas of nebular composition will primarily have a chemical composition that is governed by gas–liquid equilibria. Yoneda and Grossman (1995) and Ebel and Grossman (2000) have shown that condensate liquids of a refractory Ca–Mg–Al–silicate (CMAS) composition can be in equilibrium with forsterite and predicted that glass inclusions in chondritic olivines could represent liquids formed in dust-enriched regions with dust/gas ratio  $\approx 70$  times the ratio of the conventional solar nebula. A somewhat increased total pressure ( $P_{\text{tot}} = 10^{-3}$  atm) provides additional help to stabilize liquids.

We can envisage for that liquid an important role, namely, to facilitate condensation of the major minerals from the solar nebula gas. The results of our studies of glasses in dif-

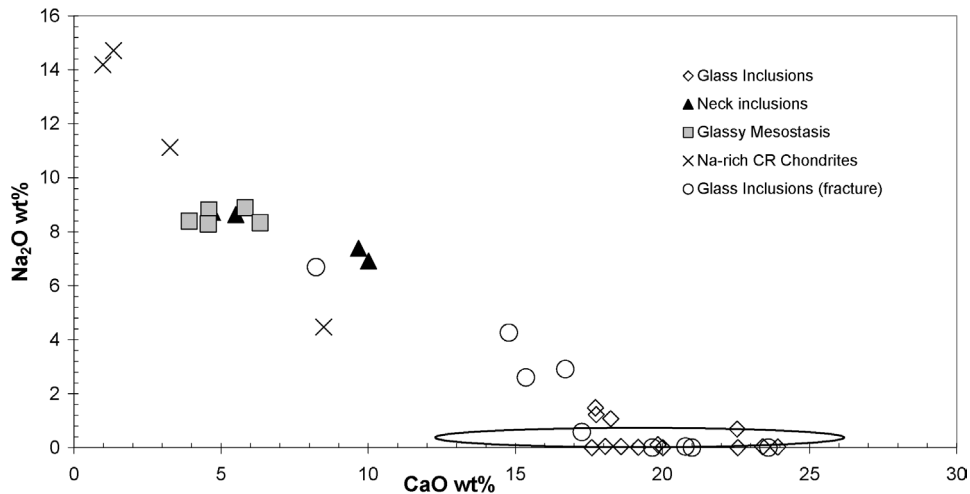


Fig. 6.  $\text{Na}_2\text{O}$  vs  $\text{CaO}$  diagram of all types of glasses from Kaba CV3 compared with glasses from CR chondrites (Varela et al., 2002). Note the high  $\text{Na}_2\text{O}$  contents in the glassy mesostasis and the neck inclusions. Glasses of glass inclusions in Kaba CV3 cover a similar compositional range as the Na-poor glasses (ellipse) in CR chondrites.

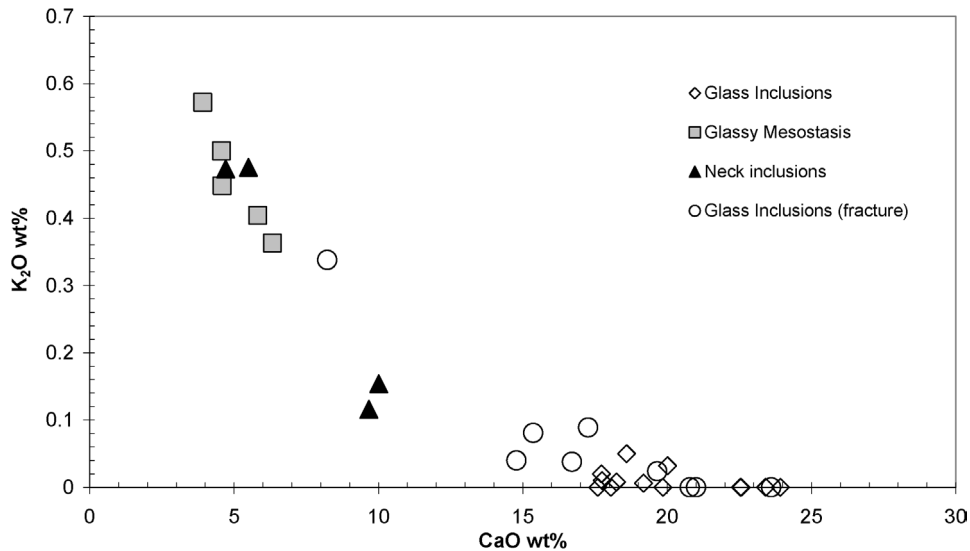
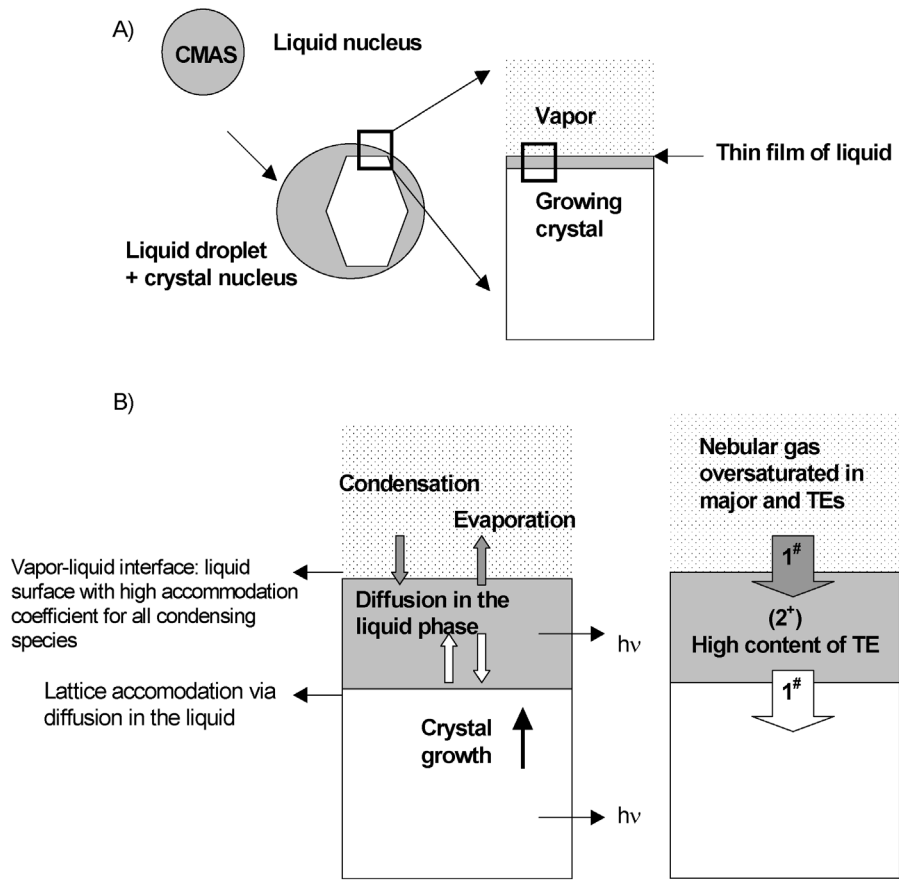


Fig. 7.  $\text{K}_2\text{O}$  vs  $\text{CaO}$  diagram of all glasses in Kaba CV3. Note the anti-correlation between these two elements in glass inclusions reached by fractures, neck inclusions and the mesostasis glasses.

ferent types of meteorites (CC, OC, EC, and achondrites, Varela et al., 2002, 2003b; Varela and Kurat, 2004) strongly support this role of nebular liquids (the glass precursors).

Our model of glass formation considers that crystals growing from the vapor need some support by a liquid to form a well ordered crystalline phase—something like the vapor–liquid–solid (VLS) growth process (see, e.g., Givargizov, 1987; Kurat et al., 1997; Varela et al., 2002) or liquid-phase epitaxy. In this process, a gas–liquid–solid condensation is involved and well ordered and large crystals can grow from the vapor with the help of a thin liquid layer bridging the vapor and the growing crystal (Figs. 8A, 8B). For developing a thin liquid interface, a total pressure higher than that of the canonical solar nebula model is needed. Once a Si–Al–Ca liquid is formed, a crystal can nucleate in this liquid (Fig. 8A). The crystal will then con-

tinue growing by taking those elements that will enter the crystal structure (e.g., Si, Mg, and O) and leave all others in the thin liquid layer. The most important function of the thin liquid layer is to accommodate condensing species without discrimination and to feed the growing crystal with the necessary elements. The elements used for growing the crystal are replenished by condensation from the vapor into the liquid (Fig. 8B). Those elements that will not easily enter the structure of the olivine, the incompatible elements like Ca, Al, and REE, will be concentrated in the vapor–crystal liquid interface. This liquid will have trace element contents which are buffered by condensation–evaporation equilibrium with the vapor which, at this stage, is oversaturated in all refractory elements (Fig. 8B). Consequently, we can expect this liquid to be rich in these elements. Because the role of this liquid is to serve as support to grow whatever phase is over-



(1<sup>#</sup>) Due to the oversaturation in the gas, the liquid receives a constant supply of those elements taken by the growing crystal.

(2<sup>\*</sup>) The liquid keeps a constantly high content of incompatible TEs.

Fig. 8. Schematic representation of the vapor–liquid–solid process in crystal growth. (A) The initial CMAS (Ca–Mg–Al–Si) liquid nucleus, the liquid droplet with the nucleated crystal and a detail of the three phases involved: vapor, a thin film of liquid and the solid (growing crystal). (B) Detail of the rectangular area in figure (A) where the four principal steps of the VLS process can be distinguished (Givargizov, 1987). (1) Condensation and evaporation; (2) the vapor–liquid interface: this is the liquid surface with high accommodation coefficient for all condensing species; (3) diffusion in the liquid; and (4) the liquid–solid interface: here takes place the incorporation of the elements into the crystal lattice.

saturated in the vapor, the trace element contents in the liquid will always be high and independent of the crystal it is associated with. Also, if this liquid can keep a memory of its formation process, one would expect its trace element pattern to show evidences of vapor fractionation. These features are just what we observe in the glasses of the CR chondrites, in those of the angrite D’Orbigny (Varela et al., 2002, 2003b) and in the glasses subject of this study. In our view, glasses can be seen as remnants of the thin liquid layer that helped crystal growth from the vapor. The process by which glass or neck inclusions in olivines are formed could be as follows: any defect at the growing surface (e.g., stacking faults, deposition of a dust particle) will produce a variation in the surface tension generating an imperfection in the growing surface to which a sample of this thin film can adhere. Subsequently it will be incorporated by the growing crystal. This stored liquid can then become a glass inclusion as the in-

terior of the growing crystal cools very fast by radiative heat transfer (e.g.,  $h\nu$ , Fig. 8B), thus quenching the liquid to glass.

As dust-enriched regions of the solar nebula also have higher oxygen partial pressures ( $fO_2$ ) and higher partial pressure of rock forming elements than the conventional nebula, they also provide the right conditions for vapor–solid exchange reactions. These oxygen-rich regions will enhance the Ca–Na exchange between the vapor and glasses, as is explained below.

#### 4.2. Glass inclusions and mesostasis

Glasses of inclusions and of metastasis have comparable chemical compositions and because of that they are assumed to contain similar information. However, they are, in fact, quite different systems. Glass inclusions carry information

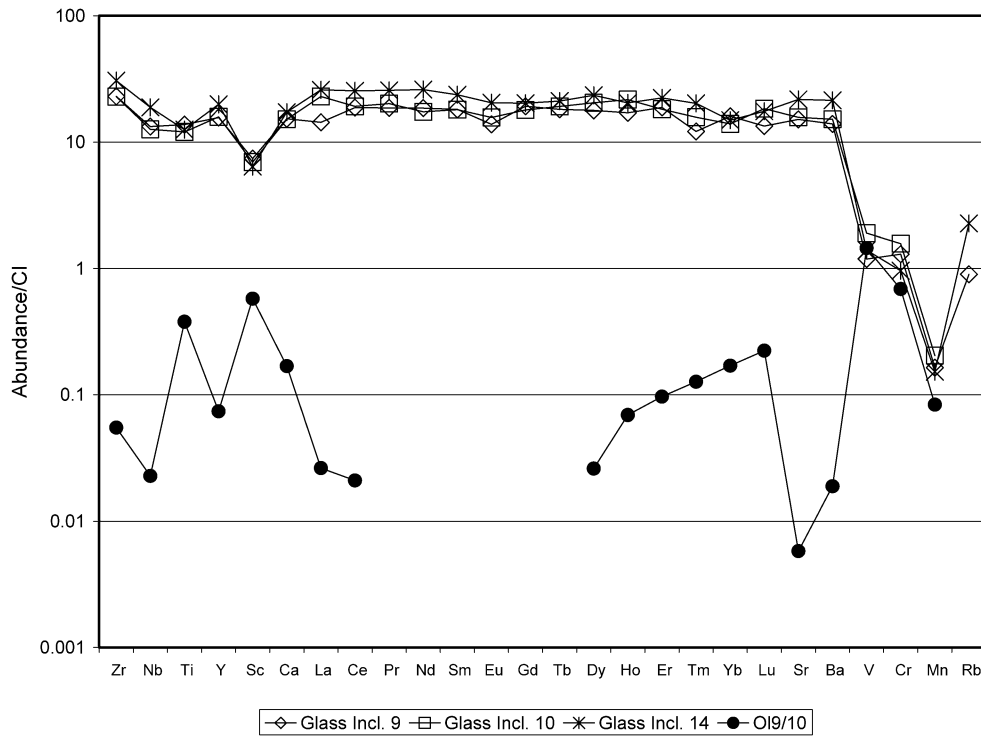


Fig. 9. CI-normalized trace element abundances in inclusion glasses 9, 10, and 14 and their host olivine. Elements in all trace element abundance plots are arranged in order of increasing volatility, except for the REE, which are arranged in order of increasing atomic number. CI abundances used here and in the following graphs are from Anders and Grevesse (1989).

on the conditions prevailing during host olivine formation. Because they are shielded by the host, they are closed systems that can retain their pristine composition and with this also information on the conditions prevailing during olivine growth. On the other hand, mesostasis glasses are irregular domains in between different crystals and are commonly in contact with several phases and the surface of the particular object. They will, therefore, behave as open systems. As a consequence, they record not only conditions during their formation but also conditions prevailing during aggregate/chondrule processing. That is, the memory of both types of glasses will cover different stages in the history of a given chondrule or aggregate.

### 4.3. Chemical variation in glasses

#### 4.3.1. Trace element abundances in inclusion and mesostasis glasses

Trace element abundances of inclusion glasses are high and typical at 10–20 × CI abundances (Figs. 9, 10). The CI-normalized abundance patterns show unfractionated refractory trace element abundances (solar relative abundances) and depletions in volatile and moderately volatile elements with respect to the refractory ones. As the abundances vary smoothly with volatility, the pattern indicates vapor fractionation. Thus, glass inclusions in the Kaba CV3 chondrite could be the product of condensation, giving additional support to our model of glass inclusion formation (Kurat et al., 1997; Varela et al., 2002). Trace element abundance patterns

of the neck inclusion and mesostasis glasses are very similar to those of glass inclusions and also indicate vapor fractionation. The only difference between these glasses is the abundance of the volatile element Rb—we shall return to this later.

If the glassy mesostasis were a residual melt, the composition of which changes as crystallization of the different phases proceeds, we must expect the trace elements in the glass to be fractionated (that is, to have non-solar relative abundances). However, no fractionation is observed.

All glasses have similar and flat, unfractionated trace element abundance patterns. Scandium, V, Mn, and Cr are depleted in all glasses with respect to the refractory trace elements. Because the degree of depletions of V, Cr, and Mn varies with the volatility of these elements and is in line with the depletion of Rb in the inclusion glass, we interpret this pattern to be due to vapor fractionation.

Glass compositions seem to be unconstrained by the phases they are in contact with and their 10–20 × CI unfractionated refractory trace element patterns appear to be an intrinsic feature. The depletion in V, Mn, and Cr observed in inclusion glasses and in the glassy mesostasis must, therefore, indicate vapor fractionation and a common origin for both glasses. That is, both glasses could likely be condensates. Then, the depletion of all glasses in V with respect to the refractory elements indicates that this condensation took place under reducing conditions or at temperatures above 1400 K, which did not allow V condensation (e.g., Lodders, 2003). The depletion of all glasses in Sc cannot be due to

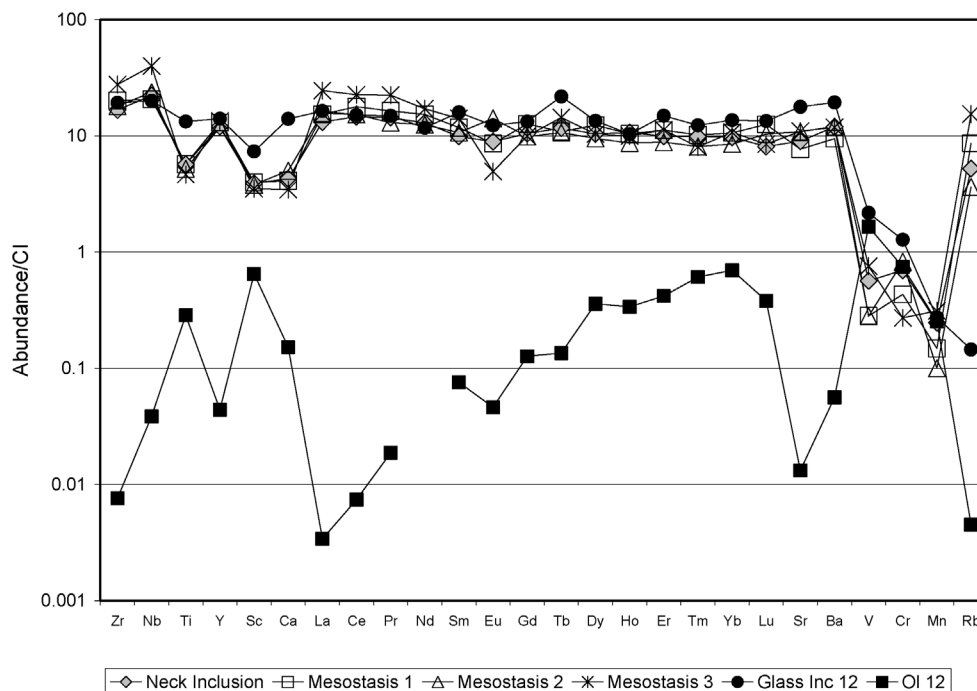


Fig. 10. CI-normalized trace element abundances in glass inclusion 12, its host olivine, neck inclusion f and the glassy mesostasis.

fractionation into the main phase olivine, as a quick view at Fig. 10 may suggest, because then the heavy rare earth elements should be depleted in the glass also with respect to the LREEs, which is not the case. Thus, the depletion in Sc could indicate separation of a refractory phase from the system before glass inclusion formation or partitioning of Sc into a volatile species. The former possible mechanism is also supported by the sub-chondritic Ti/Al ratio of these glasses. However, the undepleted abundances of Zr and Nb argue against separation of a refractory phase.

There is a major difference between the composition of inclusion glasses and the mesostasis glass: Rb is depleted with respect to the refractory elements in the inclusion glass but not in the glass of the neck inclusions and in the mesostasis glass (Figs. 9, 10). This indicates that Rb was not present in the original liquid. Consequently, it must have been added to the glass that acted as an open system and thus was able to maintain communication with the vapor until temperatures were low enough to allow the condensation of this volatile element.

#### 4.3.2. Element partitioning between glass and olivine

Trace element distribution between olivine 12 and inclusion glass 12 and the mesostasis (Ol-12/GI12 and Ol-12/mesostasis, Fig. 11) closely follows the experimental distribution coefficients  $D$  (Green, 1994; McKay and Weill, 1977; Kennedy et al., 1993; Libourel, 1999) for the elements Zr, Sr, Y, Ca, Sc, Mn, and Cr, indicating chemical equilibrium. Abundances of Nb, Sm, Gd, Ho, Er, Ti, and Yb in olivine, however, suggest disequilibrium with both glasses as they would require co-existing liquids with  $\sim 30 \times$  CI and  $\sim 200 \times$  CI abundances, much higher than the  $10 \times$  CI abun-

dances observed. Such disequilibrium has been commonly observed, is not understood yet but could be indicative of a condensation origin of the olivine that was forced to take up large quantities of trace elements (e.g., Kurat et al., 1992; Weinbruch et al., 2000) and could not re-equilibrate with the co-existing glass because of the immobility of the mostly highly charged ions involved. Trace element distribution between glasses of glass inclusions 9 and 10 and Ol-9–10 appears to follow the experimental  $D$  for the HREEs, but distributions of Ce, Zr, and Ti do not seem to be equilibrated.

The olivine-liquid trace element distribution of all glasses seems to be out of equilibrium for the refractory elements but not for the elements Mn and Cr. This result, similar to what has been observed in glasses of glass inclusions in CR chondrites and glasses in the angrite D'Orbigny, indicate that these elements are mobile and could have been introduced from the vapor by elemental exchange processes.

The mesostasis glass appears to approach equilibrium in the distribution of Ca with the olivine while glasses of inclusions are slightly low. This is likely mainly due to the fact that olivine 12 and olivine 9–10 have already seen some chemical alteration and are not anymore high-Ca olivines (CaO: 0.25 wt%, 0.30 wt%, respectively, instead of  $>0.5$  wt%), which are the primary olivines in chondrites (e.g., Steele, 1988; Kurat et al., 1989; Weinbruch et al., 2000). An unaltered high-Ca olivine such as the host of glass inclusions 6 and 7 (CaO: 0.54 wt%) is in equilibrium with the inclusion glass ( $D_{ol-gi}$ : 0.022, 0.024, respectively, as compared to the experimental equilibrium value  $D_{equ}$ : 0.025). This fact indicates that these olivines crystallized from a liquid with the chemical composition of this particular inclusion glass (Weinbruch et al., 2000;

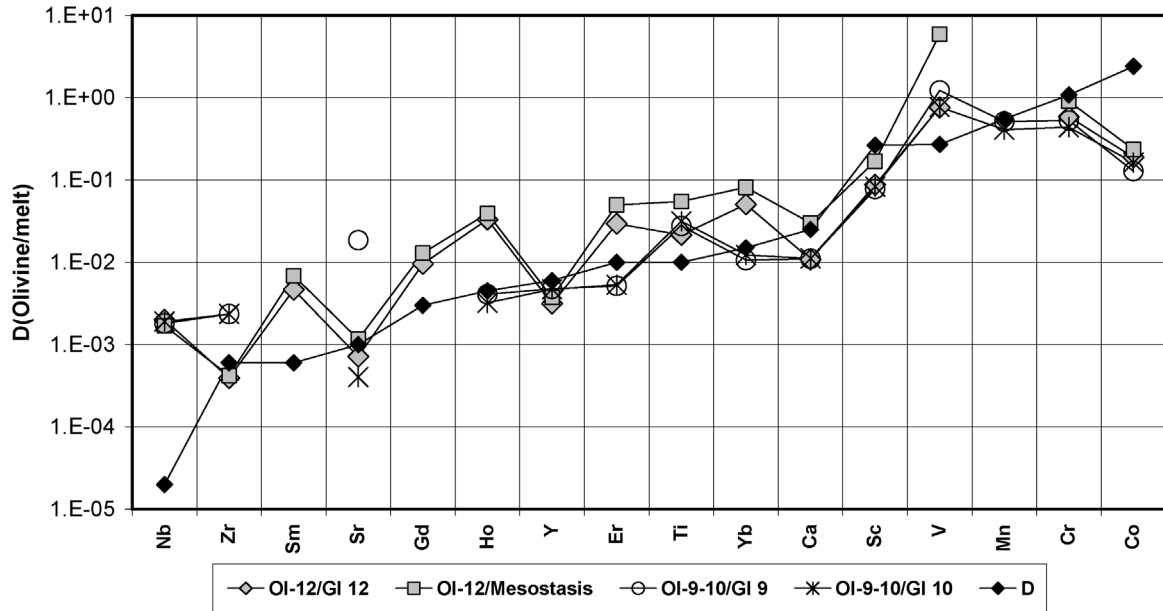


Fig. 11. Apparent trace element distribution coefficients between the olivine hosts and three glass inclusions (OI-12/GI 12, OI-9-10/GI 9, OI-9-10/GI 10) and between Olivine 12 and the co-existing mesostasis (OI-12/ Mesostasis). Olivine-liquid distribution coefficients (D) from Green (1994), McKay and Weill (1977), Kennedy et al. (1993), and Libourel (1999) are given for comparison.

Varela et al., 2002; Pack and Palme, 2003). This supports our view that the growth of olivine rich in Ca, Al and trace elements was possibly aided by the refractory liquid (represented by glass inclusions in olivine) during condensation via the VLS process (see, e.g., Givargizov, 1987; Kurat et al., 1997; Varela et al., 2002).

#### 4.3.3. Major elements: evidence for secondary elemental exchange

All glasses of the primary glass inclusions in olivine have a Si–Al–Ca-rich composition with an approximately chondritic Ca/Al ratio (Fig. 4). The mesostasis glass and the inclusion glasses have similar contents of  $\text{Al}_2\text{O}_3$  (>20 wt%) but the former has low contents of CaO: 4 to 6 wt%. To find an explanation for this CaO depletion we will compare the chemical composition of, first, glass inclusion 12 and the glassy mesostasis and, second, the different types of glasses (e.g., glass inclusions, neck inclusions) co-existing in a single host olivine.

The glass of inclusion 12 has a Si–Al–Ca-rich composition with a chondritic Ca/Al ratio and is quartz-normative, while the co-existing glassy mesostasis has low CaO and high  $\text{Na}_2\text{O}$  (~9 wt%) contents and is olivine-normative. Olivine can be grown from quartz-normative liquids, but a residual liquid cannot be olivine-normative after crystallization of olivines and low-Ca pyroxenes, as we observed. The mesostasis glass seems to be out of equilibrium with the mineral assemblage in this particular aggregate.

To explain this situation we will make some calculations. As glass inclusions are a sample of the liquid from which olivine grew, we assumed that the original composition of the mesostasis could be similar to that of the primary glass inclusion 12. As it is observed in Fig. 2, the absence of re-

action rims between the glassy mesostasis and the olivine points toward equilibrium between both phases. We calculate that we need to add 5 vol% of the host olivine to the glass until we turn the chemical composition of this glass ( $\text{SiO}_2 = 51.8$  wt%,  $\text{MgO} = 6.33$  wt%,  $\text{Al}_2\text{O}_3 = 21.8$  wt%,  $\text{CaO} = 17.3$  wt%,  $\text{FeO} = 0.28$  wt%,  $\text{Na}_2\text{O} = 1.02$  wt%) into a composition that is in equilibrium with the olivine:  $K_d[(\text{Fe}/\text{Mg})_{\text{ol}}/(\text{Fe}/\text{Mg})_{\text{Liq}}] = 0.307$  [experimental equilibrium value:  $K_d = 0.317$  (Roeder and Emslie, 1970)]. This resulting hypothetical composition is, however, quartz-normative (quartz: 6.1, plagioclase: 63.6, diopside: 22.2), different to the olivine normative one as observed. According to our calculations, if equilibrium conditions are maintained and part of the CaO content of the mixture is replaced by  $\text{Na}_2\text{O}$  (for this example we need only to add 2.4 wt%  $\text{Na}_2\text{O}$  [new glass composition: 14.95 wt% CaO and 3.42 wt%  $\text{Na}_2\text{O}$ ]), the resulting glass composition will be olivine-normative (plagioclase: 71.4, diopside: 21.3, olivine: 4.1). Thus, only the replacement of a small amount of CaO by  $\text{Na}_2\text{O}$ , possibly by a Ca–Na exchange with the vapor, can make the composition of the glassy mesostasis in the aggregate of thin section L3819 to be olivine-normative.

Another piece of evidence that supports this elemental exchange is provided by the compositions of the glasses that co-exist in a single host olivine, such as glass inclusions 5, 6, 7, 18 and the neck inclusions c and d (Table 1). The glass inclusions 5, 6, and 7 are Na-poor while glass inclusion 18, reached by three fractures, and the neck inclusions are Na-rich. That is, only those glasses that seem to have behaved as open (mesostasis and neck inclusions) or relatively open (inclusion reached by three fractures) systems had Ca replaced by Na. The fact that five of the inclusions in contact with

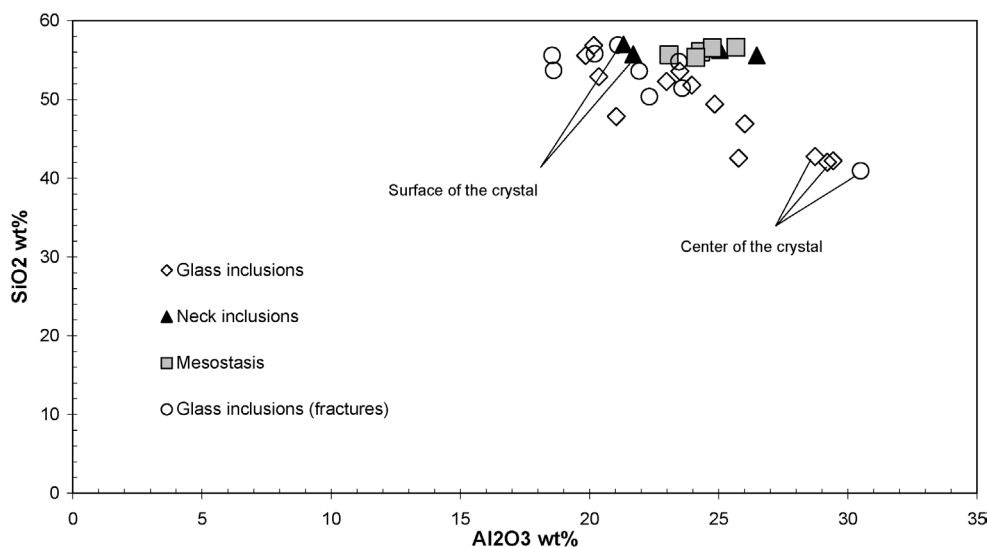


Fig. 12.  $\text{SiO}_2$  vs  $\text{Al}_2\text{O}_3$  diagram for all glasses from Kaba CV3. Note the anti-correlation for inclusion glasses. The  $\text{SiO}_2$  content of neck inclusions and mesostasis glasses is high and relatively constant. The glass inclusions located at the center of the crystal are Al-rich while the neck-inclusions are Si-rich.

fractures are Na-free just indicates that fractures were created at different times, some after the vapor–solid Ca–alkali exchange ceased. This feature, in addition to the absence of signs of devitrification in the glasses, also makes it difficult to consider that the replacement of Ca by Na could have taken place by fluid circulation (e.g., during metasomatism) in a parent body. Also, alteration of the aggregate mesostasis in a parent body seems to be excluded because we do not see any re-deposition of the Ca removed from the glass and because the matrix is too poor in alkalis ( $\text{Na}_2\text{O}$ : 0.78 wt% for Kaba matrix, Scott et al., 1988) to create a compositional potential capable to pump up to 9 wt%  $\text{Na}_2\text{O}$  into the glass.

Thus, a metasomatic exchange between Ca in a solid and Na in a vapor phase similar to that previously observed in the anorthite of Lancé basaltic objects (Kurat and Kracher, 1980), seems to be a viable mechanism. The anti-correlation between the  $\text{Na}_2\text{O}$  and CaO contents of glasses, as that observed for Na-rich glasses in CR chondrites (Fig. 6), indicates that such an exchange took place. In addition, the fact that the anti-correlation is exhibited by glasses that have acted as open systems suggests that this exchange is a secondary process that had occurred after formation of the glass inclusions. Potassium followed Na but in a less efficient way. As a consequence, the  $\text{Na}_2\text{O}/\text{K}_2\text{O}$  ratio is high (between 20 and 50). This reaction, that likely took place under sub-solidus conditions, involves exchanges of network modifier cations. Calcium that acts mainly as such a network modifier cation can be easily exchanged for alkali elements (Na, Li, Rb). One possible way this exchange can occur is following the Modifier Random Network (MRN) model of Greaves (1985). In this model the structure of the melt consist of orientationally dissimilar amorphous regions (islands) with high concentrations of network formers which contain “percolation channels” with high concentrations of network modifiers and non-bridging

oxygens that provide a high degree of mobility to these ions.

The CaO– $\text{Al}_2\text{O}_3$  anti-correlation observed in neck inclusion and mesostasis glasses (Fig. 4) indicates that also Al was somewhat mobile. The compositional diagram  $\text{SiO}_2$  vs  $\text{Al}_2\text{O}_3$  (Fig. 12) shows that, while glasses of glass inclusions exhibit an anti-correlation, those of neck inclusions and mesostasis glasses have relatively constant  $\text{SiO}_2$  contents. The glass inclusions reached by fractures have higher  $\text{SiO}_2$  contents than isolated inclusions. The compositional ranges of glass inclusions from the most Al-rich (e.g., inclusion 5, Table 1) to the most Al-poor inclusion (e.g., inclusion 17, Table 1) are as follows:  $\Delta\text{Al}_2\text{O}_3 = 12$  wt% and  $\Delta\text{SiO}_2 = 14.7$  wt%. Thus, the correlation line through glass inclusions ( $\Delta\text{SiO}_2/\Delta\text{Al}_2\text{O}_3 \sim 1.2$ ) seems to support an Si–Al exchange (mole  $\text{SiO}_2/0.5$  mole  $\text{Al}_2\text{O}_3 \sim 1.2$ ).

Also, a variation in the Si content of glasses is provided by a comparison of glasses that co-exist in a single olivine (glass inclusions 5, 6, 7 and the neck inclusions c and d, Fig. 12). The glass inclusions located at the center of the crystal (early inclusions formed at the beginning of crystal growth) are Al-rich, while the neck inclusions located close to the surface of the same crystal are Si-rich. A possible and simple way to explain this chemical variation is to increase the  $\text{SiO}_2$  content of the liquid. According to our calculations, if  $\sim 40$  wt%  $\text{SiO}_2$  is added to the glass inclusions located in the center of the crystal, the resulting glass composition ( $\sim 57$  wt%  $\text{SiO}_2$ ,  $\sim 21$  wt%  $\text{Al}_2\text{O}_3$ ) will match that of the neck inclusions. Up to this point of our studies we cannot decide which of both processes (Si–Al exchange or Si addition) could be the one that caused the silica enrichment in glasses. However, the high Si content could reflect the increased Si activity in the vapor that also lead to the formation of low-Ca pyroxene by the reaction:



Only after this reaction took place, the Ca-alkali exchange reaction could have occurred, turning the Si-normative composition of the mesostasis into an olivine-normative one.

In summary, inclusion glasses have a Si–Al–Ca-rich composition with an approximately chondritic Ca/Al ratio. Glasses of neck inclusions and mesostasis glasses are depleted in Ca and enriched in Na and Si as compared to inclusion glasses. The loss of Ca seems to be the result of a glass–vapor exchange reaction that replaced Ca by the volatile elements Na and K. This metasomatic exchange only affected glasses that acted as open systems. The gain in Si in the liquid, result of an increase in the silica activity of the system by precipitating olivine and cooling of the nebula gas, caused it to react with the olivine to form low-Ca pyroxenes and established the high SiO<sub>2</sub> content, which did not change during the final Ca-alkali exchange.

#### 4.4. A similar origin of glassy mesostasis and glass inclusions in olivines of carbonaceous chondrites

Trace element abundances of inclusion and mesostasis glasses are unfractionated and high ( $\sim 10 \times \text{CI}$ ), and show evidences of vapor fractionation. That is, glasses of glass inclusions and mesostasis seem to be the product of the same nebular event. As these glasses formed during olivine growth (glass inclusions) and during olivine aggregation (mesostasis glasses) it is probable that mesostasis glasses share the same formation process with glass inclusions in olivines of carbonaceous chondrites.

As was pointed out before, a small amount of liquid can form in specific regions of the solar nebula that helps crystal growth via a thin liquid film. If part of this layer is trapped during olivine growth, it will become a glass inclusion. During olivine growth, increase in the silica activity of the system will promote liquid formation via lowering of the liquids temperature, increasing in this way the quantity of liquid available. Thus, during aggregation of olivines part of this refractory liquid can be captured in intergranular spaces giving rise to the glassy mesostasis. Consequently, the liquid-supported condensation of major minerals in the solar nebula will also have a direct implication in the way aggregates and chondrules could have been formed (Kurat et al., 2004).

Using a thermodynamic model for ferromagnesian liquids, Ebel and Grossman (2000) concluded that all the chondrule glass compositions could represent silicate liquids in equilibrium with dust-enriched vapor within 200° of their solidus temperature at  $P_{\text{tot}} > 10^{-4}$  bar. They also pointed out that "... many chondrule glass compositions fall along bulk composition trajectories for liquids in equilibrium with cosmic gases at  $10^{-3}$  bar and dust enrichments between  $600 \times$  and  $1000 \times$ ."

From our chemical data it is likely that the Na-rich glasses were not formed from a liquid of that composition but their high Na content is the result of subsolidus metasomatic replacement of Ca by Na and K. The high partial pressure of

O prevailing in dust-enriched regions provides the right conditions for metasomatic vapor–solid exchange to proceed as oxidizing conditions are a prerequisite for mobilizing Ca as Ca(OH)<sub>2</sub> (e.g., Hashimoto, 1992).

## 5. Conclusions

In the Kaba CV3 chondrite we have studied three types of glasses: glasses of glass inclusions and neck inclusions in olivine and of glassy mesostasis. All of them seem to have formed contemporaneously. Two chemical groups of glasses can be distinguished: Al–Ca-rich (typical inclusion glasses) and Al–Na-rich (typical mesostasis and neck inclusion glasses). Trace element abundances of all glasses are unfractionated and at  $10\text{--}20 \times \text{CI}$  abundances—similar to glasses in and to bulk compositions of HED and angritic achondrites (Kurat et al., 2003a, 2003b; Varela et al., 2003a) and of group IA CAIs (Wark, 1983). The depletion in V, Mn, Li, and Cr in all glasses with respect to the refractory trace elements clearly indicates vapor fractionation and a common origin for all glasses.

The disequilibrium in trace element distribution between glasses and olivine—that are equilibrated in their Ca contents—points toward a condensation origin of the co-existing phases. Growth of olivine rich in Ca, Al and trace elements could have been supported by a thin layer of refractory liquid which has been preserved as glass inclusions in olivine (e.g., condensation via the VLS process). The aggregation of olivines could have taken place during olivine growth with capture of a part of this refractory liquid in intergranular spaces. Thus, the original composition of the glassy mesostasis must have been similar to that of the primary glass inclusions in olivines. Subsequently, the mesostasis liquid, behaving as an open system, became increasingly siliceous (without changing its trace element content) and reacted in part with co-existing olivine to form Ca-poor pyroxene. After this, liquid had been quenched to glass, that also behaved as an open system and exchanged Ca for Na (and K, Rb, Mn, Fe, ...) with the cooling vapor.

Therefore, mesostasis glasses and glasses of glass inclusions appear to be condensates and to share the same formation process: they could be considered to be remnants of the liquid interface between the growing crystal and the vapor in solar nebula regions of enhanced dust/gas ratios. As the trace element contents of the refractory liquid will be buffered by the vapor and therefore will be constant during the time of olivine growth, they will be independent of the crystal(s) they are associated with. The  $10\text{--}20 \times \text{CI}$  unfractionated trace element patterns appears to be an intrinsic feature of this refractory liquid (the glass precursor). Condensation must have occurred under initially reducing conditions from a gas from which a refractory phase had already been separated. Increasingly oxidizing conditions allowed mobilization of Ca from the mesostasis glass and its metasomatic replacement by Na under sub-solidus conditions.

## Acknowledgments

We thank Franz Brandstätter for help with the SEM. The thorough reviews of Katharina Lodders and Roger Hewins considerably improved the manuscript. Financial support was received from FWF (P13975-GEO) and the Friederike and Oskar Ermann-Fonds, Austria, from CONICET, Fundación Antorchas (P-14022/91) and SECYT (P 07-08176), Argentina, and from NASA Grant NAG5-9801.

## References

- Anders, E., Grevesse, N., 1989. Abundances of the elements: Meteoritic and solar. *Geochim. Cosmochim. Acta* 53, 197–214.
- Ebel, D., Grossman, L., 2000. Condensation in dust-enriched systems. *Geochim. Cosmochim. Acta* 64, 339–366.
- Fuchs, L.H., Olsen, E., Jensen, K.J., 1973. Mineralogy, mineral-chemistry and composition of the Murchison (C2) Meteorite. *Smithsonian Contribution to Earth Science* 10, 1–39.
- Givargizov, E.I., 1987. *Highly Anisotropic Crystals*. Reidel, Dordrecht. 394 pp.
- Gooding, J.L., Keil, K., 1981. Relative abundance of chondrule primary textural types in ordinary chondrites and their bearing on conditions of chondrule formation. *Meteoritics* 16, 17–43.
- Greaves, G.N., 1985. EXAFS and the structure of glass. *J. Non-Cryst. Solids* 71, 203–217.
- Green, T.H., 1994. Experimental studies of trace-element partitioning applicable to igneous petrogenesis—Sedona 16 years later. *Chem. Geol.* 117, 1–36.
- Grossman, L., 1972. Condensation in the primitive solar nebula. *Geochim. Cosmochim. Acta* 36, 597–619.
- Grossman, J., Wasson, J.T., 1982. Evidence of primitive nebular components in chondrules from the Chainpur chondrite. *Geochim. Cosmochim. Acta* 46, 1081–1099.
- Grossman, J.N., Wasson, J.T., 1983. Refractory precursor components of Semarkona chondrules and the fractionation of refractory elements among chondrules. *Geochim. Cosmochim. Acta* 47, 759–771.
- Hashimoto, A., 1992. The effect of H<sub>2</sub>O gas on volatiles of planet-forming major elements. I. Experimental determination of thermodynamic properties of Ca-, Al-, and Si-hydroxide gas molecules and its application to the solar nebula. *Geochim. Cosmochim. Acta* 51, 1685–1704.
- Ikeda, Y., Kimura, M., 1995. Anhydrous alteration of Allende chondrules in the solar nebula. I. Description and alteration of chondrules with known oxygen-isotopic composition. *Proc. NIPR Symp. Antarct. Meteorites* 8, 97–122.
- Kennedy, A.K., Lofgren, G.E., Wasserburg, G.J., 1993. An experimental study of trace element partitioning between olivine, orthopyroxene and melt in chondrules: Equilibrium values and kinetics effects. *Earth Planet. Sci. Lett.* 115, 177–195.
- Kurat, G., 1967. Einige Chondren aus dem Meteoriten von Mezö-Madaras. *Geochim. Cosmochim. Acta* 31, 1843–1857.
- Kurat, G., Kracher, A., 1980. Basalts in the Lancé carbonaceous chondrite. *Z. Naturforsch.* 35a, 180–190.
- Kurat, G., Mayr, M., Ntaflou, Th., Graham, A.L., 1989. Isolated olivines in the Yamato 82042 CM2 chondrite: The tracing of major condensation events in the solar nebula. *Meteoritics* 24, 35–42.
- Kurat, G., Brandstätter, F., Zinner, E., Palme, H., Spettel, B., 1992. A SIMS study of some Allende chondrules: Support for the new chondrule model. *Lunar Planet. Sci.* 23, 745–746 (abstract).
- Kurat, G., Varela, M.E., Hoppe, P., Clochiatti, R., 1997. Glass inclusions in Renazzo olivine: Condensates from the solar nebula? *Meteorit. Planet. Sci.* 32, Suppl. A76 (abstract).
- Kurat, G., Varela, M.E., Zinner, E., Maruoka, T., Brandstätter, F., 2003a. Major, minor and trace elements in some glasses from the NWA 1664 howardite. *Lunar Planet. Sci.* 34, Abstract #1733 [CD-ROM].
- Kurat, G., Varela, M.E., Zinner, E., Brandstätter, F., 2003b. Do glasses in achondritic meteorites share a common source? *Geochim. Cosmochim. Acta* 67 (S1), A 240 (abstract).
- Kurat, G., Varela, M.E., Zinner, E., Engler, A., 2004. Condensation origin model for chondrules. *Meteorit. Planet. Sci.* 39, Suppl. A57.
- Larimer, J.W., Anders, E., 1967. Chemical fractionation in meteorites. II. Abundance patterns and their interpretation. *Geochim. Cosmochim. Acta* 31, 1239–1270.
- Libourel, G., 1999. Systematics of calcium partitioning between olivine and silicate melt: Implications for melt structure and calcium content of magmatic olivines. *Contrib. Mineral. Petr.* 136, 63–80.
- Lodders, K., 2003. Solar abundances and condensation temperatures of the elements. *Astrophys. J.* 591, 1220–1247.
- McKay, G., Weill, D.F., 1977. KREEP petrogenesis revisited. *Proc. Lunar Sci. Conf.* 8, 2339–2355.
- McSween, H.Y., 1977. On the nature and origin of isolated olivine grains in carbonaceous chondrites. *Geochim. Cosmochim. Acta* 41, 411–418.
- Métrich, N., Clochiatti, R., 1989. Melt inclusions investigation of the volatile behaviour in historic basaltic magmas of Etna. *B. Volcanol.* 51, 185–198.
- Pack, A., Palme, H., 2003. Partitioning of Ca and Al between forsterite and silicate melt in dynamic systems with implications for the origin of Ca–Al-rich forsterites in primitive meteorites. *Meteorit. Planet. Sci.* 38, 1263–1281.
- Richardson, S.M., McSween, H.Y., 1978. Textural evidence bearing on the origin of isolated olivine crystals in C2 carbonaceous chondrites. *Earth Planet. Sci. Lett.* 37, 485–491.
- Roedder, E., 1981. Significance of Ca–Al-rich silicate melt inclusions in olivine crystals from the Murchison Type II carbonaceous chondrite. *B. Mineral.* 104, 339–353.
- Roeder, P.L., Emslie, R.F., 1970. Olivine-liquid equilibrium. *Contrib. Mineral. Petr.* 29, 275–289.
- Scott, E.R.D., Barber, D.J., Alexander, C.M., Hutchison, R., Peck, J.A., 1988. Primitive material surviving in chondrites: Matrix. In: Kerridge, J.F., Matthews, M.S. (Eds.), *Meteorites and the Early Solar System*. Univ. of Arizona Press, Tucson, pp. 718–745.
- Steele, I.M., 1988. Primitive material surviving in chondrites: Mineral grains. In: Kerridge, J.F., Matthews, M.S. (Eds.), *Meteorites and the Early Solar System*. Univ. of Arizona Press, Tucson, pp. 808–818.
- Varela, M.E., Métrich, N., Bonnin-Mosbah, M., Kurat, G., 2000. Carbon in glass inclusions of Allende, Vigarano, Bali and Kaba (CV3) olivines. *Geochim. Cosmochim. Acta* 64, 3923–3930.
- Varela, M.E., Kurat, G., Hoppe, P., Brandstätter, F., 2002. Chemistry of glass inclusions in olivines of the CR chondrite Renazzo, Acfer 182, and El Djouf 001. *Geochim. Cosmochim. Acta* 66, 1663–1679.
- Varela, M.E., Bonnin-Mosbah, M., Kurat, G., Gallien, J.P., 2003a. Nitrogen microanalysis of glass inclusions in chondritic olivines by nuclear reaction. *Geochim. Cosmochim. Acta* 67, 1247–1257.
- Varela, M.E., Kurat, G., Zinner, E., Métrich, N., Brandstätter, F., Ntaflou, T., Sylvester, P., 2003b. Glasses in the D'Orbigny angrite. *Geochim. Cosmochim. Acta* 67, 5027–5046.
- Varela, M.E., Kurat, G., 2004. Glasses in meteorites: A unification model. *Meteorit. Planet. Sci.* 39, Suppl. A109 (abstract).
- Wark, D.A., 1983. The Allende meteorite: Information from Ca–Al-rich inclusions on the formation and early evolution of the Solar System. Ph.D. Thesis. University of Melbourne, Melbourne, Australia, 385 pp.
- Weinbruch, S., Palme, H., Spettel, B., 2000. Refractory forsterite in primitive meteorites: Condensates from the solar nebula? *Meteorit. Planet. Sci.* 35, 161–171.
- Yoneda, S., Grossman, L., 1995. Condensation of Ca–MgO–Al<sub>2</sub>O<sub>3</sub>–SiO<sub>2</sub> liquids from cosmic gases. *Geochim. Cosmochim. Acta* 59, 3413–3444.
- Zinner, E., Crozaz, G., 1986. A method for the quantitative measurement of rare earth elements in the ion probe. *Int. J. Mass Spectrom. Ion Process.* 69, 17–38.